Bio-Nanotechnology

DOI: 10.1002/anie.200800023

# Photoactivated Biotemplated Nanoparticles as an Enzyme Mimic**

*Joseph M. Slocik, Alexander O. Govorov, and Rajesh R. Naik**

Biology provides an excellent benchmark for materials synthesis and design, assembly of highly ordered functional structures, and the potential to harness an unparalleled level of catalytic activity as exemplified by enzymes. At the cost of having exceptional substrate specificity and activity, enzymes suffer from a short shelf-life and thermal denaturation, and are difficult to separate from products, properties which are all important for practical applications. Here, we report on the synthesis of biotemplated cadmium sulfide and cadmium sulfide–platinum nanoparticles to mimic the activity of nitrate reductase in the reduction of nitrate to nitrite. Compared to native nitrate reductase, the reduction activity of CdS–Pt was found to be 23-fold higher at room temperature. At 75 °C, the activity of CdS–Pt was further increased fourfold due to enhanced electron diffusion up along the energy scale as compared to a complete loss of activity for the thermally denatured enzyme. These differences in activity and temperature dependence highlight the potential of inorganic hybrid particles over their organic counterpart. Also, notably from this work, we observe the exciton-multiplication Auger process using a simple photochemical reaction, which until now has been observed only using sophisticated ultrafast time-resolved spectroscopy.

Enzymes are extremely efficient at catalyzing a variety of reactions with high activities and yields under ambient physiological conditions. As a result, there is significant interest in utilizing enzymes for a variety of applications such as in biotransformations and as fuel-cell components.[1,2] Unfortunately, enzymes require cofactors and buffered solutions, suffer from instability due to a short shelf-life, are difficult to separate from products, and denature at elevated temperatures, thus limiting their utility for most applications. Douglas et al. constructed a protein-encapsulated platinum catalyst with $[Ru(bpy)_3]^{2+}$ for hydrogen production that mimics the enzyme hydrogenase,[3] while the well-defined photophysical properties of CdS have led to the reduction of methylviologen,[4] nitrate,[5] nitrophenol,[4] and nitrobenzene,[6] and the dehydrogenation of methanol.[7] Additionally, the properties of CdS have inspired the synthesis of many novel hybrid structures involving single-walled carbon nanotube–CdS composites for light harvesting[8] and CdS–enzyme bioconjugate complexes with cytochrome P450[9] and hydrogenase[10] for photoactivated catalysis. In each case, an electron generated in the conduction band of CdS is directly transferred to the active center of the bound enzyme and used in the reduction of the substrate, thereby eliminating an external electron carrier as required in the protein–$Pt^0$-NP/$[Ru(bpy)_3]^{2+}$ artificial hydrogenase system.

Here, we demonstrate the peptide-mediated synthesis of an integrated one-component CdS–Pt nanoparticle system as a robust inorganic mimic for the reduction of nitrate to nitrite with activity that outperforms nitrate reductase enzyme by $>23$-fold. The catalytic platform comprises photoactive CdS nanoparticles, a sacrificial peptide coat, and catalytic platinum nanoparticles (Figure 1). Importantly, the peptide interface enforces the close proximity of the platinum nanoparticles to the CdS surface for effective electron transfer, while also providing an electron donor source in the form of oxidizable tyrosine residues within the peptide for the trapped holes ($h^+$) on CdS nanocrystal. This eliminates the need for complementary electron mediators and donors.

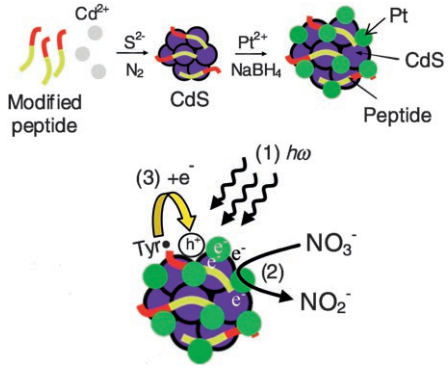


***Figure 1.*** A) Peptide-mediated synthesis of CdS–Pt using cysteine-modified peptide FlgA3C. CdS nanoparticles are first synthesized under aqueous conditions by addition of $Cd^{2+}$ and $S^{2-}$ ions to peptide. Peptide-coated CdS nanoparticles are then used to template platinum nanoparticles by addition of $Pt^{2+}$ and $NaBH_4$. B) Simplified mechanism for photoreduction of nitrate by peptide-assembled CdS–Pt nanoparticles. Excitation results in the generation of multiple excitons on CdS (1) and photoexcited electrons inside Pt which amplify the reaction. Nitrate is then reduced at the nanoparticle surface by generated electrons (2). Concertedly, the peptide coating donates electrons back to CdS to repopulate vacancies through oxidation of the tyrosine residues within peptide (3).

Using an aqueous-based approach for the synthesis of CdS,[2] we prepared a peptide-stabilized CdS nanoparticle suspension with a cysteine-modified multifunctional FlgA3C

[*] Dr. J. M. Slocik, Dr. R. R. Naik
Nanostructured & Biological Materials Branch
Materials & Manufacturing Directorate
Air Force Research Laboratory
Wright-Patterson Air Force Base, OH 45433 (USA)
Fax: (+1) 937-255-9157
E-mail: rajesh.naik@wpafb.af.mil
Prof. A. O. Govorov
Department of Physics and Astronomy, Ohio University
Athens, OH 45701 (USA)

[**] This work was supported by the Air Force Office of Scientific Research (R.R.N.) and by Ohio University (A.O.G.).

Supporting information for this article is available on the WWW under http://dx.doi.org/10.1002/anie.200800023.

peptide (-Asp-Tyr-Lys-Asp-Asp-Asp-Asp-Lys-Pro-Ala-Tyr-Ser-Ser-Gly-Ala-Pro-Pro-Met-Pro-Pro-Phe-Cys), previously used for the synthesis of Au and Au–Pd nanoparticle structures.[11,12] Advantages of using peptides as a template and passivating ligand for CdS include smaller sized particles with higher band gaps, increased stability in solution, resistance to aggregation and oxidation, surface-mediated photophysical phenomena, and a functional handle on the surface, as has been demonstrated with cysteine, phytochelatin peptide analogues, and glutathione ligands.[4,13] Synthesis of CdS nanoparticles using FlgA3C yielded a typical absorption maximum at 280 nm and a broad fluorescence emission at ca. 580 nm, characteristic of biomimetically synthesized CdS particles (Figure 2).[4,14–16] IR analysis confirmed the presence of the peptide coat on CdS by the absence of an S–H stretch, a shifted amide I band at 1665 $cm^{-1}$, and an amide II band at 1575 $cm^{-1}$ relative to the free peptide (see Figure S1 in the Supporting Information), while the TEM micrographs showed characteristic lattice fringes for CdS particles and sizes approaching 3 nm.

Given that the FlgA3C peptide contains multiple amino acid side chains capable of metal binding, we used the peptide surface of CdS as a template for the synthesis of platinum nanoparticles. Based on our previous synthesis of bimetallic Au–Pd nanoparticles, the platinum salt precursor solution ($K_2PtCl_4$) was added to CdS nanoparticles coated with the FlgA3C peptide and incubated to promote binding at the peptide interface, then followed by reduction with sodium borohydride. This resulted in a decrease in the absorbance shoulder at 280 nm for CdS and an increase at longer wavelengths by UV/Vis (Figure 2A). In addition, the fluorescence of CdS was completely quenched by the formation of platinum nanoparticles (Figure 2B), suggesting the platinum nanoparticles reside near the CdS surface, since quenching efficiency is dependent upon the separation distance and is well known with other metals.[17–20] Analysis by TEM confirmed a close spatial arrangement of 1.5 nm sized Pt particles around a central CdS nanoparticle that appear to be arranged in chains (Figure 2C). Comparatively, the particle size of platinum is consistent with other reported platinum nanoparticles which ranged in size from 3 nm to 17 nm depending on the stabilizing ligand (amine or thiol).[21] When assembled, the CdS–Pt nanoparticle complex was found to have a diameter of 13 nm by TEM, and 15 nm by sedimentation on a CPS disk centrifuge particle-size analyzer which is based on the size-dependent sedimentation of particles in liquids. The Pt nanoparticles appeared mostly spheroidal and exhibited minimal aggregation unlike platinum particles with mercaptosuccinic acid, citrate, or amino acids.[21,22] From the micrograph, it appears that the majority (> 80 %) of Pt nanoparticles are associated with CdS.

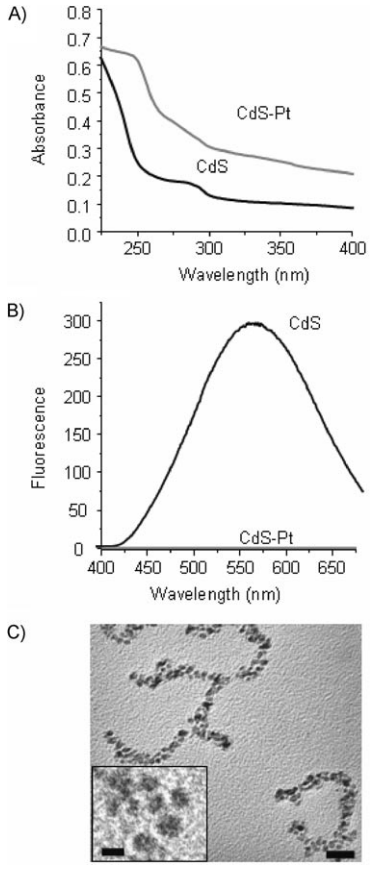


***Figure 2.*** Characterization of peptide-coated CdS (black line) and CdS–Pt nanoparticles (gray line). A) UV/Vis spectra of biotemplated CdS and CdS–Pt nanoparticle solution. B) Fluorescence spectra obtained at an excitation of 270 nm. C) TEM micrograph of CdS–Pt structures (scale bar 13 nm). Inset: Arrangement of the nanoparticles (scale bar 4 nm) (see Figure S2 in the Supporting Information).

The peptide assembly of Pt nanoparticles with CdS affords an active platform for achieving enzyme-like activity in the reduction of nitrate. Consequently, we examined nitrate reduction by excitation of CdS or CdS–Pt nanoparticles at various excitation wavelengths or by the preparation of the nitrate reductase enzyme (plus cofactor) in the presence of 40 μM nitrate for 2.5 h. The amount of $NO_2^-$ formed either photocatalytically or enzymatically was quantitated using a standard fluorometric assay to yield activity plots (Figure 3). For CdS and CdS–Pt nanoparticles there was a significant increase in the amount of $NO_2^-$ formed after 90 min of excitation at 250 nm. In contrast, little or no nitrite was detected in the absence of excitation over time (Figure 3, ●). Furthermore, the CdS–Pt nanoparticle system was found to be more active in the formation of $NO_2^-$ when compared to CdS nanoparticles due to the addition of platinum which serves to amplify the reaction. When the standard enzyme assay protocol for nitrate reductase was used, a linear increase in enzyme activity over time with a rate equal to 14.8 μmol-($NO_2^-$) g(enzyme)$^{-1}$ $min^{-1}$ was observed (Figure 3, ■, and Figure S3 in the Supporting Information). When compared to nitrate reductase, the activity of the CdS–Pt nanoparticle system was 23-fold higher (303.2 μmol($NO_2^-$) g-(CdS)$^{-1}$ $min^{-1}$), while the nitrate reduction activity of CdS nanoparticles was comparatively lower (186.6 μmol($NO_2^-$)), but higher than that of the enzyme. Recently, it was reported that the addition of Pt colloids to bulk CdS led to an increase in the yield of azoxybenzene;[6] however, formation of Pt nanoparticles that were not coupled to the CdS nanoparticle, resulting in unassembled Pt particles, failed to further increase the nitrate reduction activity of the cysteine-coated

  

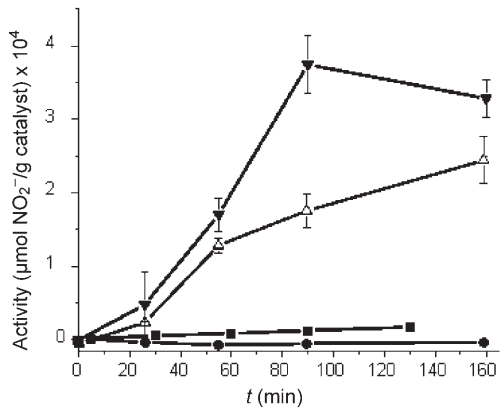


***Figure 3.*** Plot of nitrate reduction activity over time measured by the formation of nitrite. Activity of biotemplated CdS–Pt (▼), CdS nanoparticles (△) when excited at 250 nm, nitrate reductase (cofactor added), enzyme (■), and CdS–Pt nanoparticles without excitation (●). Nitrite concentrations were determined by incubating 30 μL aliquots from enzyme or CdS assay at specified time intervals with 2,3-diaminonaphthalene (in 0.68 M HCl) in phosphate buffer pH 6.8 for 15 min. This was excited at 370 nm, measured at 431 nm for fluorescence intensity, and quantified using a standard $NO_2^-$ concentration plot.

CdS nanoparticle (CdS(Cys)). Therefore, this indicates the importance of controlling the proximity of Pt and CdS particles to enhance activity (Figure S4 in the Supporting Information).

To better understand the physical and chemical processes inside the CdS–Pt photoexcited complex, we examined the energy diagram (Figure 4 A). The important parameters are the work function of Pt ($E_{Pt}$) and affinity of CdS ($E_{CdS}$). Since the optical selection rules in nanocrystals are relaxed, the incident photons can create excited electrons with the energy intervals: $E_{CdS} < E < E_{CdS}-E_{g,CdS}+\hbar\omega$ (inside CdS) and $E_{Pt} < E < E_{Pt}-E_{g,CdS}+\hbar\omega$ (inside Pt); here $\hbar\omega$ and $E_{g,CdS}$ are the incident-photon energy and CdS band gap, respectively. Optically excited electrons can either relax back to the Fermi energy or are trapped in localized states at the surfaces of nanocrystals. The trapped optically excited electrons can be then involved in the slow chemical reaction occurring at the nanocrystal surface. The chemical transformation [Eq. (1)] develops with release of energy, 0.7 eV per one $NO_2^-$ molecule.

$$NO_3^- + H_2O + 2e^- \rightarrow NO_2^- + 2OH^- \quad (1)$$

This means that the electrons with negative energies can be used for this reaction. Since two electrons are needed, the threshold for the electron energy is $E_{th} = -0.35$ eV. In other words, trapped electrons with the energies around −0.35 eV or higher can take part in the reaction. We emphasize again that, since the chemical reactions at the surface of CdS nanoparticle happens over a longer timescale, the photoexcited electrons need to be trapped at the surface states of CdS. We now assume that the probability that an electron is used for the chemical reaction decreases exponentially away from the threshold of −0.35 eV: $P = P_0 \exp[-(E_{th}-E)/\Delta]$ where the energy $E = 0$ corresponds to the vacuum energy.

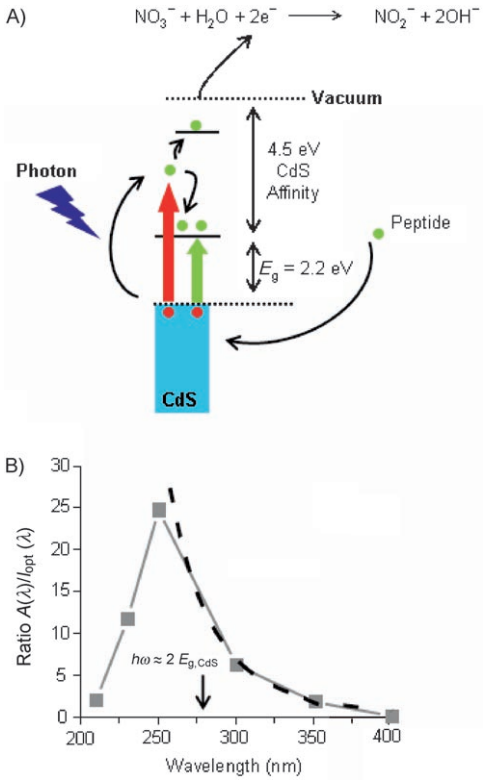


***Figure 4.*** Physical model of photoreduction of nitrate by CdS nanoparticles. A) Energy diagram illustrating optical, relaxation, and chemical processes. An optically excited electron–hole pair can relax or be used for the chemical reaction. The fast relaxation process comes from Auger multiplication of excitons. B) The ratio of chemical activity and absorption rates as a function of the excitation wavelength. The maximum of the ratio is close to the threshold of Auger multiplication process. The dashed curve shows an exponential fit.

Then, the total number of electrons trapped in CdS and involved in the chemical reaction can be evaluated by Equation (2), where $I_{opt}(\omega)$ is the rate of optical absorption.

$$N_{CdS} \propto \int_{E_{c,CdS}}^{E_{c,CdS}-E_g+\hbar\omega} P(E)\mathrm{d}E\, I_{opt}(\omega) \quad (2)$$

We also assume that electrons are trapped uniformly over energy. After integration we obtain the ratio $N_{CdS}(\omega)/I_{opt}(\omega) \propto \exp(\hbar\omega/\Delta)$. The theoretical ratio $N_{CdS}(\omega)/I_{opt}(\omega)$ can be compared with the experimental ratio $A_{CdS}(\omega)/I_{opt}(\omega)$ (Figure 4 B); here $A_{CdS}(\omega)$ is the chemical activity for the CdS nanocrystal. We see that the theoretical function $N_{CdS}(\omega)/I_{opt}(\omega)$ provides a rather good fit to the experiment using $\Delta = 0.5$ eV for long wavelengths. In experiments with Pt nanoparticles alone, we do not observe nitrate reduction activity. The Pt nanoparticle serves as amplifier of the reaction. Its work function is 5.65 eV (this number is smaller than the CdS affinity, 6.7 eV) and electrons photoexcited inside Pt can penetrate CdS and enhance the reaction.

Interestingly, the chemical activity strongly decreases at shorter wavelenghts ($\lambda < 250$ nm). The maximum of $A_{CdS}(\lambda)/I_{opt}(\lambda)$ is not far from the wavelength $\lambda = 288$ nm that

  

corresponds to the condition $\hbar\omega = 2E_{g,CdS}$. We can suggest that this behavior is due to the fast Auger processes inside the CdS-NP that lead to fast relaxation of the photoexcited electron. Under the condition $\hbar\omega > 2E_{g,CdS}$, the photoexcited electron-pair is able to create two excitons with single-exciton energies about $2E_{g,CdS}$ (Figure 4A). Therefore, the photoexcited electron would rather relax than be trapped on the surface states in CdS. We note that, so far, the exciton-multiplication Auger processes have been observed only with ultrafast picosecond spectroscopy which is a rather sophisticated experimental method.[23] Here we can observe this effect using a very different, much simpler method of photochemical spectroscopy.

Finally we determined the effect of temperature on the catalytic activity of the CdS–Pt nanoparticle system (Figure 5). Since optically excited electrons are below the reaction threshold, increased temperatures can facilitate the reaction, enhancing electron diffusion up along the energy scale. The nitrate reduction acivity of the CdS–Pt nanoparticle system shows very strong enhancement in activity as seen at 75 °C (Figure 5), most likely due to more photoexcited electrons that become available for the reaction. In contrast, the nitrate reductase enzyme showed no nitrate reduction activity at 75 °C (Figure 5). The main conclusion from the above discussion is that the chemical activity and the ratio $A_{CdS}(\omega)/I_{opt}(\omega)$ strongly increase with the photon energy since more trapped high-energy electrons become available for the chemical reaction; simultaneously, the strong decrease of $A_{CdS}(\omega)/I_{opt}(\omega)$ at high energies may come from the Auger processes.

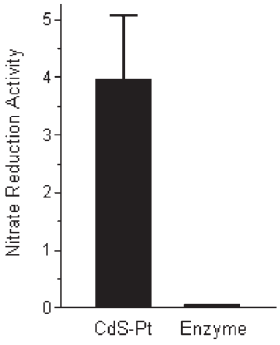


***Figure 5.*** Nitrate reduction activity as a function of temperature. Activity of CdS–Pt (exc. 250 nm) and enzyme at 75 °C (black bars). The nitrate reduction activity was measured as the ratio of reduction activity at 75 °C to that at 25 °C.

The FlgA3C peptide coat plays a supporting role in the reaction since a separate sacrificial electron donor is not required for the reaction to occur. Presumably, an electron is sacrificed from the FlgA3C peptide coating to repopulate the trapped holes on CdS through oxidation of the two available tyrosine residues. The electron-donating ability of the peptide is well supported by the known redox properties of tyrosine in a number of biochemical processes such as in photosystem II ($Tyr_z$ to $P680^+$) and in the potentiated reduction of gold salts.[24,25] To further support the role of tyrosine as a donor from FlgA3C, we examined the UV/Vis spectrum both before and after catalysis and explored the effect of exogenous electron donors hexatyrosine (YYYYYY) and tetraaspartic acid (DDDD) peptide on the methyl viologen ($MV^{2+}$) quenched fluorescence of CdS(Cys) at a fixed $MV^{2+}$ concentration of 1.0 μM. A suitable electron donor will donate electrons to CdS which in turn will increase the fluorescence of CdS. Addition of DDDD (0–2.0 μM) resulted in no change to the fluorescence of CdS(Cys), indicative of a poor electron donor; whereas with the addition of YYYYYY, the CdS(Cys) fluorescence recovered with increasing concentrations of peptide donor (Figure S5 in the Supporting Information). Additionally, we compared the fluorescence quenching of CdS(FlgA3C) and CdS(Cys) by increasing the concentration of $MV^{2+}$ (0–2.0 μM). For cysteine-capped CdS particles, the fluorescence was quenched immediately after only 0.2 μM of methyl viologen, whereas for CdS(FlgA3C), the fluorescence of CdS was found to be relatively stable and showed decreased fluorescence only at higher cocentrations of $MV^{2+}$ (>1 μM). Based on these considerations, there comes a point where the peptide is depleted of available electrons for CdS and activity diminishes. As a result, the nitrate reduction activity of the CdS–Pt nanoparticles decreased after repeated use (Figure S6 in the Supporting Information).

The combination of peptide-coated CdS with Pt provides an excellent platform for achieving increased catalytic activity, while also eliminating the need for electron mediators, exogenous sacrificial electron donors, or even enzymes for certain applications. By comparison, the biotemplated nanoparticles exhibit enhanced activity, are optically activated, and can be used at elevated temperatures. The ability to use a peptide template to structurally encode for the components of the nanoparticle system is a powerful concept that would be useful in the development of inorganic catalyst systems.

## Experimental Section

Synthesis of FlgA3C peptide-coated CdS: 2 mg of lyophilized FlgA3C peptide (New England Peptide Inc.) was dissolved in 100 μL of deionized water and 900 μL of 0.25 M Tris buffer pH 9.2 in a 3 mL glass vial with a micro magnetic stir bar, then purged with $N_2$ for 10 min. 25 μL of 35 mM $CdCl_2$ in 0.01 M HCl (Sigma–Aldrich) was added to peptide solution under $N_2$ and incubated for 30 min. After formation of $Cd^{2+}$–peptide complex, 25 μL of 0.1 M $Na_2S$ was slowly added under $N_2$. The glass vial was covered in foil and the reaction mixture stirred on magnetic stir plate for 18 h. After 18 h, the solution had turned yellow indicating formation of peptide-coated CdS. Particles were purified from excess peptide by repeated ethanol precipitation, whereby 30 mL of cold absolute ethanol was added to crude CdS nanoparticles, refrigerated to promote precipitation, and centrifuged at 14000 rpm to obtain a pellet of CdS. This was repeated two more times; and upon final centrifugation, the pellet was dissolved in 200 μL of deionized water.

Synthesis of CdS–Pt nanoparticles: 10 μL of purified CdS-(FlgA3C) particles was added to 610 μL of deionized water. This was followed by addition of 2 μL of $K_2PtCl_4$ (0.1 M) and subsequent incubation for 30 min. After 30 min, CdS-peptide bound $Pt^{2+}$ was reduced by 10 μL of $NaBH_4$ (0.1 M) for 3 h.

Characterization: Particles were characterized by UV/Vis on a Varian Cary 500 Scan UV/Vis/NIR spectrophotometer, FTIR using a Perkin–Elmer FTIR spectrometer SPECTRUM 2000 with an AutoI-

  

mage microscope and double-sided polished silicon wafer, and fluorescence on a Cary eclipse fluorometer. TEM was performed using a Phillips CM200 transmission electron microscope with the field emission gun operating at 200 kV. Samples were prepared by pipetting 10 μL of solution onto a 3 mm copper grid coated with carbon substrate (Ted Pella). Sizes were also determined with a CPS particle size analyzer model DC24000 at 24000 rpm on a sucrose gradient prepared on a gradient maker with 8% and 24% (w/v) sucrose solutions. Particles were calibrated against a 377 nm polyvinylchloride standard provided with the instrument.

Nitrate reduction assay: 100 μL of 200 μM $NaNO_3$ (in 20 mM phosphate buffer pH 7.4) was added to 400 μL of 20 mM phosphate buffer pH 7.4 in a 500 μL quartz cuvette (Starna) with 20 μL of peptide-coated CdS–Pt nanoparticles. Particles in the presence of nitrate were irradiated on a Cary Eclipse fluorometer with excitation and emission slits set to 20 nm and 10 nm, respectively, over 180 min at several different excitation wavelengths (200, 250, 290, 350, and 400 nm). During the period of irradiation, products were sampled at several time points by removing 30 μL aliquots.

Quantitation of nitrite: Each 30 μL aliqout from assay was added to 470 μL of 20 mM potassium phosphate buffer pH 7.4 and 10 μL of 2,3-diaminonaphthalene (50 $\mu g\,mL^{-1}$ in 0.62 M HCl) (Cayman Chemical). The mixture was incubated for 20 min and measured for fluorescence at 431 nm at an excitation wavelength of 375 nm with excitation and emission slits set to 5 nm and 10 nm, respectively. Nitrite concentrations were determined from a standard plot of known nitrite concentrations.

Received: January 3, 2008
Published online: June 13, 2008

**Keywords:** biomimetics · biomineralization · heterogeneous catalysis · hybrid nanoparticles · peptides

[1] K. A. Vincent, J. A. Cracknell, J. R. Clark, M. Ludwig, O. Lenz, B. Friedrich, F. A. Armstrong, *Chem. Commun.* **2006**, 5033–5035.
[2] C. R. Johnson, *Acc. Chem. Res.* **1998**, *31*, 333–341.
[3] Z. Varpness, J. W. Peters, M. Young, T. Douglas, *Nano. Lett.* **2005**, *5*, 2306–2309.
[4] G. Spreitzer, J. M. Whitling, J. D. Madura, D. W. Wright, *Chem. Commun.* **2000**, 209–210.
[5] B. A. Korgel, H. G. Monbouquette, *J. Phys. Chem. B* **1997**, *101*, 5010–5017.
[6] B. Pal, T. Torimoto, K.-i. Okazaki, B. Ohtani, *Chem. Commun.* **2007**, 483–485.
[7] B. Pal, T. Tsukasa, K. Iwasaki, T. Shibayama, H. Takahashi, B. Ohtani, *J. Phys. Chem. B* **2004**, *108*, 18670–18674.
[8] I. Robel, B. A. Bunker, P. V. Kamat, *Adv. Mater.* **2005**, *17*, 2458–2463.
[9] B. I. Ipe, C. M. Niemeyer, *Angew. Chem.* **2006**, *118*, 519–522; *Angew. Chem. Int. Ed.* **2006**, *45*, 504–507.
[10] A. I. Nedoluzhko, I. A. Shumilin, V. V. Nikandrov, *J. Phys. Chem.* **1996**, *100*, 17544–17550.
[11] J. M. Slocik, M. O. Stone, R. R. Naik, *Small* **2005**, *1*, 1048–1052.
[12] J. M. Slocik, R. R. Naik, *Adv. Mater.* **2006**, *18*, 1988–1992.
[13] J. M. Tsay, S. Doose, F. Pinaud, S. Weiss, *J. Phys. Chem. B* **2005**, *109*, 1669–1674.
[14] W. Bae, R. K. Mehra, *J. Inorg. Biochem.* **1998**, *69*, 33–43.
[15] L. Nguyen, R. Kho, W. Bae, R. K. Mehra, *Chemosphere* **1999**, *38*, 155–173.
[16] C. T. Dameron, B. R. Smith, D. R. Winge, *J. Biol. Chem.* **1989**, *264*, 17355–17360.
[17] J. R. Lakowicz, *Anal. Biochem.* **2005**, *337*, 171–194.
[18] L. Dyadyusha, H. Yin, S. Jaiswal, T. Brown, J. J. Baumberg, F. P. Booy, T. Melvin, *Chem. Commun.* **2005**, 3201–3203.
[19] A. O. Govorov, G. W. Bryant, W. Zhang, T. Skeini, J. Lee, N. A. Kotov, J. M. Slocik, R. R. Naik, *Nano Lett.* **2006**, *6*, 984–994.
[20] J. M. Slocik, A. O. Govorov, R. R. Naik, *Supramol. Chem.* **2006**, *18*, 415–421.
[21] J. M. Slocik, D. W. Wright, *Biomacromolecules* **2003**, *4*, 1135–1141.
[22] S. Chen, K. Kimura, *J. Phys. Chem. B* **2001**, *105*, 5397–5403.
[23] R. D. Schaller, V. I. Klimov, *Phys. Rev. Lett.* **2004**, *92*, 186601.
[24] M. Sjödin, S. Styring, B. Åkermark, L. Sun, L. Hammarström, *J. Am. Chem. Soc.* **2000**, *122*, 3932–3936.
[25] Y. Zhou, W. Chen, H. Itoh, K. Naka, Q. Ni, H. Yamane, Y. Chujo, *Chem. Commun.* **2001**, 2518–2519.

  